



PCCP

**Tetra-arm poly(ethylene glycol) gels with highly concentrated sulfolane-based electrolytes exhibiting high Li-ion transference numbers**

Journal:	<i>Physical Chemistry Chemical Physics</i>
Manuscript ID	CP-COM-04-2023-001928.R1
Article Type:	Communication
Date Submitted by the Author:	12-Jun-2023
Complete List of Authors:	Tasaki, Natsumi; Yokohama National University, Department of Chemistry and Biotechnology Ugata, Yosuke; Yokohama National University, Department of Chemistry and Life Science Hashimoto, Kei; Gifu University, Department of Chemistry and Biomolecular Science Kokubo, Hisashi; Yokohama Kokuritsu Daigaku Ueno, Kazuhide; Yokohama National University, Department of Chemistry and Biotechnology Watanabe, Masayoshi; Yokohama National University, Chemistry and Biotechnology Dokko, Kaoru; Yokohama National University, Department of Chemistry and Biotechnology

SCHOLARONE™  
Manuscripts

## COMMUNICATION

## Tetra-arm poly(ethylene glycol) gels with highly concentrated sulfolane-based electrolytes exhibiting high Li-ion transference numbers

Received 00th January 20xx,  
Accepted 00th January 20xx

DOI: 10.1039/x0xx00000x

Natsumi Tasaki,<sup>a</sup> Yosuke Ugata,<sup>a,b</sup> Kei Hashimoto,<sup>c</sup> Hisashi Kokubo,<sup>a</sup> Kazuhide Ueno,<sup>a,b</sup> Masayoshi Watanabe,<sup>b</sup> and Kaoru Dokko<sup>\*a,b</sup>

**We demonstrate that tetra-arm poly(ethylene glycol) gels containing highly concentrated sulfolane-based electrolytes exhibit high Li<sup>+</sup> transference numbers. The low polymer concentration and homogeneous polymer network in the gel electrolyte are useful in achieving both mechanical reliability and high Li<sup>+</sup> transport ability.**

Lithium-ion batteries (LIBs) are energy-storage devices with high energy densities that are widely used in various applications ranging from portable electronic devices to electric vehicles. Flammable organic liquid electrolytes are widely used in LIBs. Non-flammable and solid electrolytes are desirable to achieve LIBs with high safety. Sulfolane (SL) is a thermally stable and fire-retardant solvent that can dissolve high-concentration Li salts.<sup>1,2</sup> Highly concentrated electrolytes (HCEs) containing Li salts of over 3 mol dm<sup>-3</sup> have recently attracted increased attention for their attractive properties, which include high thermal stability and wide electrochemical windows.<sup>3-7</sup> We previously reported that SL-based HCEs exhibit a Li<sup>+</sup>-ion-hopping conduction mechanism.<sup>8-10</sup> A unique solvation structure in which different Li<sup>+</sup> ions are cross-linked by the SL solvent and anions is formed in SL-based HCEs. In the crosslinked structure, Li<sup>+</sup> ions dynamically exchange and diffuse/migrate faster than ligands (SL solvent and anions), leading to high Li<sup>+</sup>-ion transference numbers ( $t_{\text{Li}^+}^{\text{abc}}$ , >0.5). A high  $t_{\text{Li}^+}^{\text{abc}}$  effectively suppresses concentration polarisation during the high-rate charging/discharging of LIBs.<sup>8,10</sup>

HCE gelation can prevent the leakage of liquids and improve the safety of LIBs. Liquid electrolytes are incorporated into the polymer networks of polymer gel electrolytes. The ionic

conductivity of a gel electrolyte is generally lower than that of the parent liquid electrolyte. However, high polymer concentrations (typically >20 wt%) are required to prepare self-standing and mechanically reliable gel electrolytes. The use of tetra-arm poly(ethylene glycol) (TPEG) has been proposed to achieve both high ionic conductivity and mechanical toughness in gel electrolytes.<sup>11-13</sup> TPEG gels obtained by the end-coupling reaction of two symmetrical TPEGs with different terminals exhibit excellent mechanical properties.<sup>14,15</sup> TPEG forms a homogeneous polymer network, which allows the resulting gels to uniformly disperse external stresses. Consequently, TPEG gels possess excellent mechanical toughness even at low polymer concentrations (<10 wt%). In this study, we prepared novel self-standing TPEG-based gel membranes containing a high-concentration LiN(SO<sub>2</sub>CF<sub>3</sub>)<sub>2</sub> (LiTFSA)/SL electrolyte and elucidated the solvation structure of Li<sup>+</sup> in the gels. We then

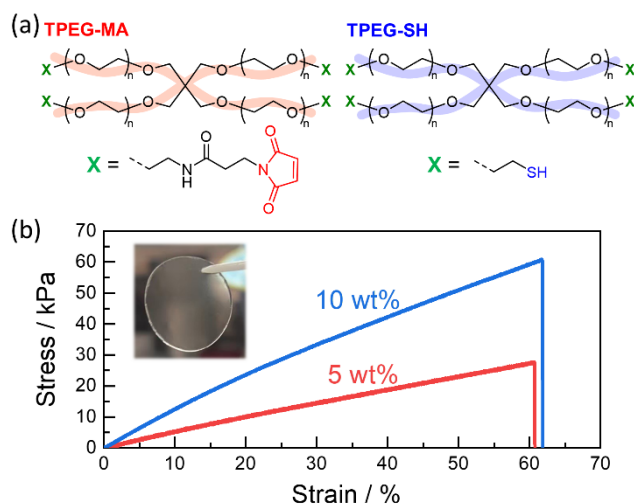


**Fig. 1** (a) Chemical structures of TPEG-MA and TPEG-SH. (b) Stress-strain curves of 5 and 10 wt% LPD-TPEG gels at 30 °C. Inset: Photograph of the 5 wt% LPD-TPEG gel.

<sup>a</sup> Department of Chemistry and Life Science, Yokohama National University, 79-5 Tokiwadai, Hodogaya-ku, Yokohama 240-8501, Japan.

<sup>b</sup> Advanced Chemical Energy Research Centre, Institute of Advanced Sciences, Yokohama National University, 79-5 Tokiwadai, Hodogaya-ku, Yokohama 240-8501, Japan.

<sup>c</sup> Department of Chemistry and Biomolecular Science, Gifu University, 1-1 Yanagido, Gifu 501-1193, Japan.

Electronic Supplementary Information (ESI) available. See DOI: 10.1039/x0xx00000x

characterised the mechanical, ion-transport, and electrochemical properties of the gels. Finally, we fabricated a Li/LiCoO<sub>2</sub> cell using the TPEG gel electrolyte and demonstrated its operation.

TPEG prepolymers with thiol (SH) and maleimide (MA) ends (10 kDa; each arm had a molecular weight of 2.5 kDa) were used for the gelation of the SL-based HCE (Fig. 1a). PEG chains have strong solvation ability and form complexes with Li<sup>+</sup>.<sup>13</sup> Therefore, the TPEG prepolymers were pre-doped with LiTfSA to maintain the solvation structure of Li<sup>+</sup> in the parent SL-based HCE. The detailed procedure for preparing LiTfSA-pre-doped TPEG prepolymers (LPD-TPEG) is described in the Electronic Supplementary Information (ESI). The molar ratio of [LiTfSA]/[EO], where EO is the ether oxygen of the TPEG prepolymer, was controlled at 1:5. The LPD-TPEG prepolymers were dissolved in SL-based HCEs ([LiTfSA]/[SL] molar ratio = 1:2) in different vials in an Ar-filled glove box to prepare homogeneous solutions. Two solutions of the prepolymers LPD-TPEG-SH and LPD-TPEG-MA were mixed and cast into a Teflon mould to obtain an LPD-TPEG gel membrane (500 μm thick), and the Michael addition reaction between the SH and MA ends was allowed to proceed at 80 °C. The progress of the gelation reaction was confirmed by time-dependent UV spectroscopy. In the case of the LPD-TPEG gel with a polymer concentration of 5 wt%, the gelation reaction was nearly completed after 168 h at 80 °C (Fig. S1, ESI). The reaction efficiency was estimated from the peak intensity of the MA terminal at approximately 300 nm and found to be 91% (Fig. S2, ESI). For comparison, TPEG gels without LiTfSA pre-doping were prepared in a similar manner. The molar ratios of LiTfSA/SL in the 5 and 10 wt% LPD-TPEG gels are shown in Table S1.

The prepared LPD-TPEG gels were thermally stable and showed low vapour pressures at temperatures lower than 180 °C (Fig. S3, ESI). The gel membranes are self standing, flexible, and stretchable. The stress-strain curves of the 5 and 10 wt% LPD-TPEG gel membranes are shown in Fig. 1b. The Young's modulus of the membranes increased with increasing polymer concentration. Even at a low polymer concentration of 5 wt%, the Young's modulus, fracture stress, and fracture strain of the membranes were 53 kPa, 28 kPa, and 61%, respectively. The strain-dependent variations of the storage modulus *G'*, loss modulus *G''*, and loss tangent (*tan δ*) of the 5 wt% LPD-TPEG gel are shown in Fig. S4 (ESI). The 5 wt% LPD-TPEG gel had a high breaking strain of 400% and *G'* of 17 kPa, which are similar to those of previously reported TPEG gels.<sup>13</sup> The *tan δ* value reflects the homogeneity of a polymer network. The *tan δ* of the 5 wt% LPD-TPEG gel was estimated to be  $2.6 \times 10^{-4}$  at a strain of  $\gamma = 1\%$ . This value is comparable with that of other TPEG gels ( $\sim 10^{-4}$ ), indicating that a homogeneous TPEG network was formed within the gel.<sup>12,13</sup>

The Raman spectra of the gels and [LiTfSA]/[SL] = 1:2 solution (without the polymer) are shown in Fig. 2. The peak corresponding to the S-N-S stretching vibrations of TfSA anions can be observed in the range 740–750 cm<sup>-1</sup>. This peak is known to be sensitive to the complex formation of TfSA with Li<sup>+</sup>.<sup>16–18</sup> According to the literature,<sup>17,18</sup> TfSA anions not coordinated to Li<sup>+</sup> show a band in the range 739–742 cm<sup>-1</sup>, whereas TfSA

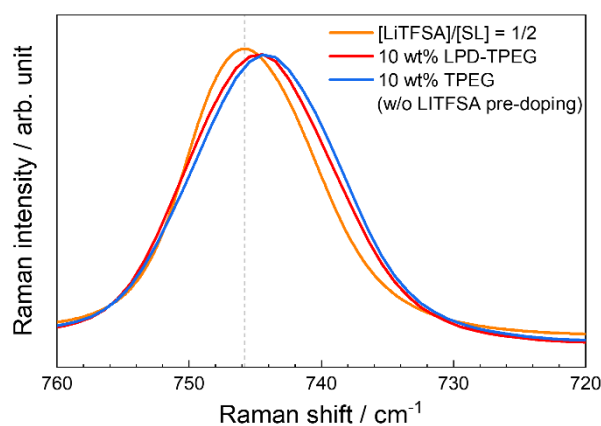


Fig. 2 Raman spectra of TPEG gels and the [LiTfSA]/[SL] = 1:2 solution at 30 °C.

anions directly bound to Li<sup>+</sup> to form contact ion pairs (CIPs) and ionic aggregates (AGGs) exhibit bands in the range of 745–755 cm<sup>-1</sup>. The S-N-S vibration peak of the [LiTfSA]/[SL] = 1:2 solution was observed at 746 cm<sup>-1</sup>, thus suggesting that the TfSA anions formed CIPs and AGGs in the solution.<sup>17,18</sup> In the case of the 10 wt.% LPD-TPEG gel, the TfSA peak shifted slightly towards a lower wavenumber compared with that of the [LiTfSA]/[SL] = 1:2 solution. For comparison, the spectrum of the 10 wt% TPEG gel (without LiTfSA pre-doping) is shown in Fig. 2. The S-N-S vibration peak shifted towards an even lower wavenumber in the TPEG gel (without LiTfSA pre-doping). These results indicate that gelation using TPEG changes the coordination structure of Li<sup>+</sup>. PEG is well known to form complexes with Li<sup>+</sup> owing to the strong electron-donating ability of the ether oxygen.<sup>19</sup> Gutman's donor number (DN) is a good metric of electron-donating ability (Lewis basicity). The DNs of ether solvents (such as tetrahydrofuran and dimethoxyethane) are in the range 16–20 kcal mol<sup>-1</sup>, while the DNs of TfSA anions and SL are 5.4 and 14.8 kcal mol<sup>-1</sup>, respectively.<sup>20,21</sup> Therefore, Li<sup>+</sup> ions (Lewis acid) preferably coordinate to the PEG chain (strong Lewis base) in the gel. In the case of the TPEG gel, the gelation and complex formation of the Li<sup>+</sup> and PEG chains proceed simultaneously in the [LiTfSA]/[SL] = 1:2 solution, and the dissociation of Li<sup>+</sup>-TfSA<sup>-</sup> partially occurs. However, in the case of the 10 wt% TPEG gel (without LiTfSA pre-doping), the [LiTfSA]/[EO] molar ratio is 1:1.32. The typical coordination number of Li<sup>+</sup> is in the range of 4–6;<sup>22,23</sup> therefore, the coordination number cannot be fulfilled

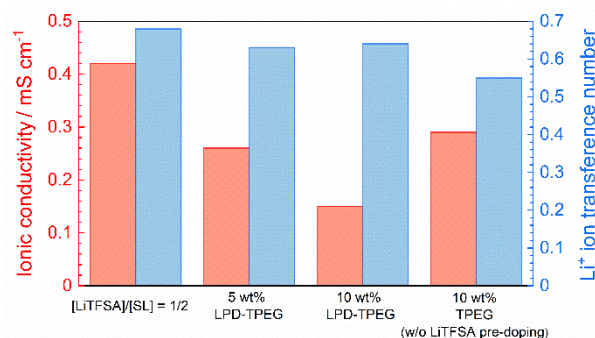
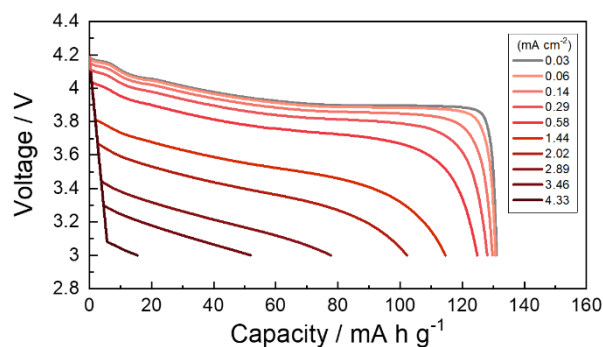


Fig. 3 Ionic conductivities and Li<sup>+</sup> transference numbers of the electrolytes at 30 °C.

even if all ether oxygen atoms are involved in the coordination of  $\text{Li}^+$  ions in the gel. Consequently, the populations of CIPs and AGGs remain high after TPEG gelation. The PEG chains in the LPD-TPEG gels are coordinated to  $\text{Li}^+$  ions even prior to gelation, and the coordination structure of  $\text{Li}^+$  in the  $[\text{LiTFSA}]/[\text{SL}] = 1:2$  solution is rather maintained during gelation.

The ionic conductivities and  $t_{\text{Li}}^{\text{abc}}$  of the gels and  $[\text{LiTFSA}]/[\text{SL}] = 1:2$  solution are shown in **Fig. 3**. The ionic conductivity of the LPD-TPEG gel was lower than that of the  $[\text{LiTFSA}]/[\text{SL}] = 1:2$  solution and decreased with increasing polymer concentration. The decrease in the ionic conductivity of the LPD-TPEG gel electrolyte is attributable to its lower charge-carrier number compared with that of the  $[\text{LiTFSA}]/[\text{SL}] = 1:2$  solution as well as the polymer chains impeding ion migration. The ionic conductivity of the 10 wt% TPEG gel (without LiTFSA pre-doping) was higher than that of the LPD-TPEG gel electrolyte because of the dissociation of  $\text{Li}^+$ -TFSA<sup>-</sup> owing to  $\text{Li}^+$ -PEG complex formation during gelation (vide supra), resulting in a higher charge-carrier number compared with that in the LPD-TPEG gels. The  $t_{\text{Li}}^{\text{abc}}$  values were estimated under anion-blocking conditions using Li/Li symmetric cells (**Fig. S5**, ESI).<sup>24,25</sup> The gels composed of 5 and 10 wt% LPD-TPEG exhibited  $t_{\text{Li}}^{\text{abc}}$  values of 0.63 and 0.64, respectively, which are comparable with that of the  $[\text{LiTFSA}]/[\text{SL}] = 1:2$  solution (0.68) (**Fig. 3**).<sup>26</sup> However, the  $t_{\text{Li}}^{\text{abc}}$  of the 10 wt% TPEG gel (without LiTFSA pre-doping) was 0.55, which is considerably lower than that of the  $[\text{LiTFSA}]/[\text{SL}] = 1:2$  electrolyte.  $\text{Li}^+$  hopping conduction occurs in highly concentrated SL-based electrolytes; thus, the mobility of  $\text{Li}^+$  is higher than that of the anion.<sup>19,20,33</sup> This phenomenon results in relatively high  $t_{\text{Li}}^{\text{abc}}$  values of over 0.6 compared with that in conventional electrolytes containing ca.  $1 \text{ mol dm}^{-3}$  Li salt, the  $t_{\text{Li}}^{\text{abc}}$  values of which are  $\sim 0.3$ .<sup>10</sup> In the case of the 10 wt% TPEG gel (without LiTFSA pre-doping),  $\text{Li}^+$  and PEG chains form long-lived complexes owing to the chelate effect,<sup>27,28</sup> and the PEG chains trap  $\text{Li}^+$  ions, thereby lowering the mobility of  $\text{Li}^+$  relative to that of the TFSA anion and the  $t_{\text{Li}}^{\text{abc}}$  in the gel. However, in the case of the LPD-TPEG gels, the PEG chains are already coordinated to  $\text{Li}^+$  ions (vide supra), and the coordination structure of  $\text{Li}^+$  in the  $[\text{LiTFSA}]/[\text{SL}] = 1:2$  solution is maintained within the polymer matrix, thus preventing the reduction of  $t_{\text{Li}}^{\text{abc}}$ .

The LPD-TPEG gels exhibited wide electrochemical windows similar to those of the  $[\text{LiTFSA}]/[\text{SL}] = 1:2$  electrolyte (**Fig. S6** and **S7**, ESI). PEG oxidatively decomposes at electrode potentials higher than 4 V vs. Li;<sup>29</sup> therefore, ether-based electrolytes have not been utilised in 4 V class Lithium batteries. However, as shown in **Fig. S6** (ESI), the oxidative current was suppressed at potentials lower than 4.5 V. The improvement in the oxidative stability of PEG is due to the lowering of the HOMO energy level of the its chains owing to complexation with  $\text{Li}^+$ .<sup>30</sup> SL solvent is oxidatively stable but reductively decomposes on Li metal.<sup>31–33</sup> However, the reductive decomposition of SL can be mitigated by increasing the Li salt concentration. The mitigation of reductive decomposition can be ascribed to the TFSA-derived passivation layer on the Li metal,<sup>34</sup> which enables reversible Li deposition/dissolution (**Fig. S7**, ESI).



**Fig. 4** Discharge curves of a Li/LiCo<sub>2</sub> cell with 5 wt% LPD-TPEG at 30 °C.

Finally, a 5 wt% LPD-TPEG gel electrolyte was tested in a 4 V class cell with a Li metal anode and LiCo<sub>2</sub> cathode. The galvanostatic charge–discharge curves of the cell measured at a low current density of  $29 \mu\text{A cm}^{-2}$  are shown in **Fig. S8** (ESI). The cell exhibited a discharge capacity of  $135 \text{ mAh g}^{-1}$  based on the mass of LiCo<sub>2</sub>, which is close to the theoretical capacity ( $\sim 140 \text{ mAh g}^{-1}$ ) of the electrochemical reaction of  $\text{LiCoO}_2/\text{Li}_{0.5}\text{CoO}_2$  in the voltage range of 3.0–4.2 V. The cell could be operated reversibly and cycled over 50 charge–discharge cycles, indicating that severe side reactions did not occur at the anode and cathode because of the wide electrochemical window of the gel. The Coulombic efficiency of the cell during the initial several cycles was  $\sim 96\%$  and increased gradually up to 99% with increasing cycle number. An excess amount of Li metal was used as the anode in the cell; therefore, a Coulombic efficiency of less than 100% implies that irreversible reactions occurred at the LiCo<sub>2</sub> cathode. The small amount of water in the gel electrolyte as an impurity may decompose at the LiCo<sub>2</sub> cathode during the first several cycles. To investigate the effects of transport properties on battery performance, we recorded the discharge curves of a  $[\text{Li} | \text{LPD-TPEG gel} | \text{LiCo}_2]$  cell at various current densities (**Fig. 4**). The discharge voltage decreased with increasing current density, which can be attributed to the electrolyte and interfacial resistances at the cathode and anode. The discharge capacity remained nearly constant at current densities lower than  $0.3 \text{ mA cm}^{-2}$  and decreased gradually at current densities higher than  $0.5 \text{ mA cm}^{-2}$ . However, 60% of the theoretical capacity of LiCo<sub>2</sub> was maintained, even at a relatively high current density of  $2.89 \text{ mA cm}^{-2}$ . The discharge capacity decreased with increasing current density because of the limited diffusion of  $\text{Li}^+$  ions in the gel electrolyte.<sup>35,36</sup> When discharging at a high current density, the Li salt concentration increases and decreases near the anode and cathode, respectively, and a concentration gradient is formed across the gel electrolyte membrane, causing concentration polarisation. This phenomenon also lowers the cell voltage to the cutoff voltage (3.0 V) before the full cell capacity is achieved. We previously reported the discharge rate capability of a Li/LiCo<sub>2</sub> cell with a high-concentration electrolyte of  $2.75 \text{ mol dm}^{-3}$  LiTFSA/tetraglyme (G4).<sup>36</sup> The cell with the G4-based electrolyte could not discharge at current densities higher than  $2.0 \text{ mA cm}^{-2}$  despite its higher ionic conductivity ( $1.6 \text{ mS cm}^{-1}$ ) compared with that of the LPD-TPEG

gel electrolyte ( $0.26 \text{ mS cm}^{-1}$ ). The enhanced rate capability of the cell with the LPD-TPEG gel electrolyte can be attributed to its much higher  $t_{\text{Li}^{\text{abc}}}$  (0.63) compared with that of the G4-based electrolyte ( $t_{\text{Li}^{\text{abc}}} = 0.03$ ).<sup>26</sup> A high  $t_{\text{Li}^{\text{abc}}}$  effectively suppresses the concentration gradient in the electrolyte, thereby decreasing the concentration overpotential in the cell.<sup>35,37</sup> Consequently, the cell with the LPD-TPEG gel electrolyte exhibited better rate capability than that with the G4-based electrolyte. Note that the gel membrane, at  $500 \mu\text{m}$ , was thicker than typical porous polyolefin separators ( $\sim 20 \mu\text{m}$ ) used in practical LIBs. The  $\text{Li}^+$  diffusion-limiting current density can be increased by employing a thin electrolyte membrane (i.e., a thin diffusion layer). Further improvements in rate capability can be achieved by using a thinner LPD-TPEG gel membrane.

In summary, this study demonstrates that gel electrolyte membranes comprising SL-based HCEs and a homogeneous TPEG polymer network exhibit high  $t_{\text{Li}^{\text{abc}}}$ . A self-standing gel electrolyte could be prepared with a low polymer concentration of 5 wt% to alleviate the decrease in ionic conductivity compared with that of the parent HCE owing to the presence of polymer chains. Pre-doping of TPEG with LITFSA effectively maintained the  $\text{Li}^+$  solvation structure in the parent HCE during gelation, resulting in a high  $t_{\text{Li}^{\text{abc}}}$  ( $\sim 0.6$ ) and the wide electrochemical window of the gel. A Li/LiCoO<sub>2</sub> cell with the TPEG gel electrolyte membrane could discharge at a current density of  $2.9 \text{ mA cm}^{-2}$  despite its high thickness of  $500 \mu\text{m}$  and the relatively low ionic conductivity ( $0.26 \text{ mS cm}^{-1}$ ) of the gel electrolyte. The high  $t_{\text{Li}^{\text{abc}}}$  of the gel electrolyte effectively suppressed concentration polarisation during discharge at high current densities. This study provides a new design concept for gel electrolytes for thermally stable high-energy-density high-power LIBs.

This study was partially supported by JSPS KAKENHI (Grant Nos. JP19H05813, JP21H04697, JP22H00340, and JP23K13822) from the Japan Society for the Promotion of Science (JSPS) and JST ALCA-SPRING (Grant Number JPMJAL1301), Japan.

## Conflicts of interest

There are no conflicts to declare.

## Notes and references

- 1 K. Xu and C. A. Angell, *J. Electrochem. Soc.*, 2002, **149**, A920–A926.
- 2 A. Abouimrane, I. Belharouak and K. Amine, *Electrochem. Commun.*, 2009, **11**, 1073–1076.
- 3 Y. Yamada and A. Yamada, *J. Electrochem. Soc.*, 2015, **162**, A2406–A2423.
- 4 Y. Yamada, J. Wang, S. Ko, E. Watanabe and A. Yamada, *Nat. Energy*, 2019, **4**, 269–280.
- 5 O. Borodin, J. Self, K. A. Persson, C. Wang and K. Xu, *Joule*, 2020, **4**, 69–100.
- 6 M. Li, C. Wang, Z. Chen, K. Xu and J. Lu, *Chem. Rev.*, 2020, **120**, 6783–6819.
- 7 Y. Ugata, K. Shigenobu, R. Tatara, K. Ueno, M. Watanabe and K. Dokko, *Phys. Chem. Chem. Phys.*, 2021, **23**, 21419–21436.
- 8 K. Dokko, D. Watanabe, Y. Ugata, M. L. Thomas, S. Tsuzuki, W. Shinoda, K. Hashimoto, K. Ueno, Y. Umabayashi and M. Watanabe, *J. Phys. Chem. B*, 2018, **122**, 10736–10745.
- 9 A. Nakanishi, K. Ueno, D. Watanabe, Y. Ugata, Y. Matsumae, J. Liu, M. L. Thomas, K. Dokko and M. Watanabe, *J. Phys. Chem. C*, 2019, **123**, 14229–14238.
- 10 Y. Ugata, Y. Chen, S. Sasagawa, K. Ueno, M. Watanabe, H. Mita, J. Shimura, M. Nagamine and K. Dokko, *J. Phys. Chem. C*, 2022, **126**, 10024–10034.
- 11 K. Fujii, H. Asai, T. Ueki, T. Sakai, S. Imaizumi, U. Il Chung, M. Watanabe and M. Shibayama, *Soft Matter*, 2012, **8**, 1756–1759.
- 12 S. Ishii, H. Kokubo, K. Hashimoto, S. Imaizumi and M. Watanabe, *Macromolecules*, 2017, **50**, 2906–2915.
- 13 K. Hashimoto, R. Tatara, K. Ueno, K. Dokko and M. Watanabe, *J. Electrochem. Soc.*, 2021, **168**, 090538.
- 14 T. Sakai, T. Matsunaga, Y. Yamamoto, C. Ito, R. Yoshida, S. Suzuki, N. Sasaki, M. Shibayama and U. Il Chung, *Macromolecules*, 2008, **41**, 5379–5384.
- 15 T. Matsunaga, T. Sakai, Y. Akagi, U. Il Chung and M. Shibayama, *Macromolecules*, 2009, **42**, 1344–1351.
- 16 Y. Umabayashi, T. Mitsugi, S. Fukuda, T. Fujimori, K. Fujii, R. Kanzaki, M. Takeuchi and S. I. Ishiguro, *J. Phys. Chem. B*, 2007, **111**, 13028–13032.
- 17 D. M. Seo, P. D. Boyle, R. D. Sommer, J. S. Daubert, O. Borodin and W. A. Henderson, *J. Phys. Chem. B*, 2014, **118**, 13601–13608.
- 18 W. A. Henderson, M. L. Helm, D. M. Seo, P. C. Trulove, H. C. De Long and O. Borodin, *J. Electrochem. Soc.*, 2022, **169**, 060515.
- 19 Z. Xue, D. He and X. Xie, *J. Mater. Chem. A*, 2015, **3**, 19218–19253.
- 20 W. Linert, A. Camard, M. Armand and C. Michot, *Coord. Chem. Rev.*, 2002, **226**, 137–141.
- 21 K. Izutsu, *Electrochemistry in Nonaqueous Solutions*, Wiley-VCH Verlag GmbH & Co. KGaA, Weinheim, Germany, 2nd edn., 2009.
- 22 S.-A. Hyodo and K. Okabayashi, *Electrochim. Acta*, 1989, **34**, 1551–1556.
- 23 Y. Kameda, Y. Umabayashi, M. Takeuchi, M. A. Wahab, S. Fukuda, S. Ishiguro, M. Sasaki, Y. Amo and T. Usuki, *J. Phys. Chem. B*, 2007, **111**, 6104–6109.
- 24 J. Evans, C. A. Vincent and P. G. Bruce, *Polymer (Guildf.)*, 1987, **28**, 2324–2328.
- 25 M. D. Galluzzo, J. A. Maslyn, D. B. Shah and N. P. Balsara, *J. Chem. Phys.*, 2019, **151**, 020901.
- 26 K. Shigenobu, K. Dokko, M. Watanabe and K. Ueno, *Phys. Chem. Chem. Phys.*, 2020, **22**, 15214–15221.
- 27 F. Müller-Plathe and W. F. Van Gunsteren, *J. Chem. Phys.*, 1995, **103**, 4745–4756.
- 28 C. Zhang, K. Ueno, A. Yamazaki, K. Yoshida, H. Moon, T. Mandai, Y. Umabayashi, K. Dokko and M. Watanabe, *J. Phys. Chem. B*, 2014, **118**, 5144–5153.
- 29 S. Seki, Y. Kobayashi, H. Miyashiro, A. Yamanaka, Y. Mita and T. Iwahori, *J. Power Sources*, 2005, **146**, 741–744.
- 30 K. Yoshida, M. Nakamura, Y. Kazue, N. Tachikawa, S. Tsuzuki, S. Seki, K. Dokko and M. Watanabe, *J. Am. Chem. Soc.*, 2011, **133**, 13121–13129.
- 31 S. Tan, Y. J. Ji, Z. R. Zhang and Y. Yang, *ChemPhysChem*, 2014, **15**, 1956–1969.
- 32 X. Ren, S. Chen, H. Lee, D. Mei, M. H. Engelhard, S. D. Burton, W. Zhao, J. Zheng, Q. Li, M. S. Ding, M. Schroeder, J. Alvarado, K. Xu, Y. S. Meng, J. Liu, J. G. Zhang and W. Xu, *Chem*, 2018, **4**, 1877–1892.
- 33 Y. Ugata, R. Tatara, T. Mandai, K. Ueno, M. Watanabe and K. Dokko, *ACS Appl. Energy Mater.*, 2021, **4**, 1851–1859.
- 34 Y. Yamada, K. Furukawa, K. Sodeyama, K. Kikuchi, M. Yaegashi, Y. Tateyama and A. Yamada, *J. Am. Chem. Soc.*, 2014, **136**, 5039–5046.
- 35 M. Doyle, T. F. Fuller and J. Newman, *Electrochim. Acta*, 1994, **39**, 2073–2081.
- 36 K. Yoshida, M. Tsuchiya, N. Tachikawa, K. Dokko and M. Watanabe, *J. Electrochem. Soc.*, 2012, **159**, A1005–A1012.
- 37 K. M. Diederichsen, E. J. McShane and B. D. McCloskey, *ACS Energy Lett.*, 2017, **2**, 2563–2575.